

Role of Multidetector Computed Tomography Coronary Angiography in Evaluation of Coronary Bifurcation Angles as a Predictor of Coronary Artery Disease

Rabab Mohamed Abdelhay*, Samar Mohamed Shehata,

Sara Emad eldin Abdellatif, Mohamad Gamal Nada, Hanan A. Bahaaeldin

Department of Radiology, Faculty of Medicine, Zagazig University, Zagazig, Egypt

*Corresponding author: Rabab Mohamed Abdelhay, **Mobile:** (+20) 01204592842, **E-Mail :** rababbarakat.rm@gmail.com

ABSTRACT

Background: The common and potentially fatal disorder known as coronary artery disease (CAD) is characterised by turbulent and sluggish blood flow at the coronary artery bifurcation site, particularly at broader angles. Curved multiplanar reformat (CMPR) and 3D volume rendering (3D VR) techniques could help in prediction of CAD. **Objective:** The aim of the current study was to evaluate of the capability of Multi-detector CT (MDCT) coronary angiography to quantify coronary bifurcation angles for early preventative treatment or preprocedural planning for coronary intervention. **Patients and methods:** Using a 128-detectors scanner, 60 patients with typical or atypical chest discomfort or failed catheterization received MDCT coronary angiography to characterise coronary anatomy. Coronary bifurcation angles were calculated using specialised software and post-processing methods for correlation with CAD severity. **Results:** Compared to the 3D VR approach, the CMPR technique revealed wider values of coronary bifurcation angles. However, Bland-Altman plots showed that both methods may be alternatively used. Because a wider angle was linked to a greater degree of stenosis, LAD-LCX angle differed significantly between individuals with significant and nonsignificant CAD. **Conclusion:** Measurements of various coronary bifurcation angles, particularly the LAD-LCX angle, which is thought to be a predictor for CAD, can be made using MDCT coronary angiographic examination with CMPR and 3D VR methods. More plaques are likely to form when the angle is wider.

Keywords: Coronary artery disease, Bifurcation angle, CMPR, 3D VR, Coronary computed tomography angiography.

INTRODUCTION

In order to replace traditional coronary artery angiography (CCA), since the early 1990s, a number of non-invasive imaging techniques have been developed for visualizing the coronary arteries [1]. These methods were initially seemed insufficient for widespread clinical use, despite the fact that they have produced encouraging outcomes. Electron-beam computed tomography (EBCT), as well as Magnetic resonance (MR), are two examples of modern imaging technologies that are still frequently employed [2]. The improved performance of 128-slice CT equipment and the advent of multi-slice computed tomography coronary angiography (MSCT-CA) have provided a viable alternative to conventional CCA for the diagnosis of coronary artery disease [3].

Utilization of coronary computed tomography angiography (CCTA) imaging non-invasive technique showed good sensitivity and negative predictive value that is frequently used to diagnose coronary stenosis. Additionally, utilizing various post-processing methods such maximum intensity projection (MIP), multiplanar reformatted images (MPR), curved multiplanar reformat (CMPR), and 3D VR make CCTA precisely estimate coronary bifurcation angles [4].

The distribution and make-up of plaques may be greatly influenced by the hemodynamic flow patterns that are affected by the three-dimensional (3D) geometry of coronary artery bifurcations [4]. Furthermore, Coronary bifurcation angle has been linked to the formation of plaques in the side branches of coronary arteries due to the turbulent and sluggish flow there [5].

Plaque start in the arterial system may be affected by hemodynamic changes brought on by variations in wall shear stress according to coronary bifurcation angle,

there is growing clinical concern for angles between the LAD and the left circumflex coronary artery (LCX) as well as the angles between the left main coronary artery (LM) and the left anterior descending coronary artery (LAD) [6].

Interventional cardiologists have emphasized the importance of the coronary bifurcation angle in coronary artery disease (CAD) diagnosis and treatment. Accurate measurement of the bifurcation angle is essential for the successful placement of coronary stents and the prevention of restenosis and stent thrombosis [5].

The aim of the current study was to evaluate of the capability of Multi-detector CT (MDCT) coronary angiography to quantify coronary bifurcation angles for early preventative treatment or preprocedural planning for coronary intervention.

PATIENTS AND METHODS

In the current study, we stuck to validate our findings according to Strengthening the Reporting of Observational Studies in Epidemiology (STROBE).

A total of 60 adult patients took part in this retrospective single-center study between July 2022 and December 2022. Patients were evaluated by the Cardiology Department and then referred to the Radiology Department for CCTA.

Participants were considered eligible for the present study if they had either typical or atypical chest discomfort or if they were scheduled for coronary revascularization treatments that needed a precise assessment of the coronary artery tree. Patients included whither they had previously undergone CCA or not.

Patients of any age or gender who arrived with typical or atypical chest discomfort, preprocedural planning, or

who had previously undergone unsuccessful cardiac catheterization operations were eligible for inclusion in the present retrospective study.

We excluded patients with abnormal renal function, patients with hypersensitivity to contrast media, pregnant women, people with morbid obesity, people who had had post-PCI or CABG surgeries, people with poor image quality, hemodynamic instability, people who could not hold their breath for 12 seconds, people with tachycardia of more than 70 beats per minute or who had an arrhythmia.

All patients had a full medical history review prior to the CT coronary angiography assessment to determine their coronary artery disease risk factors and to look into any prior chest discomfort, revascularization treatments, cyanosis, or conventional coronary angiography. For controlling control heart rate to 65 beats per minute for the best image quality, patient preparation included both respiratory training to achieve a single breath hold for 12 seconds and beta-blocker treatment one day prior to the examination. ECG gating was employed to simultaneously gather the patient's ECG trace and the CT scan data after an intravenous line was created in the right antecubital vein.

The CT coronary angiography exam was performed using a 128-detector scanner (Philips Healthcare Ingenuity, Philips Medical System, Best, Netherlands). After obtaining a scanogram and calcium score, the exam was considered complete if both values were greater than 500. Bolus tracing was utilized to inject 80–100 ml of non-ionic contrast media at a rate of 5–6 ml/sec using a dual-head Medrad stellant injector pump. The contrast medium was then flushed out of the right side of the heart with a 50 ml saline chaser bolus.

Semi-prospective CTA (phases: 40-80%) was performed from the carina to 1 cm below the diaphragm while the patient held their breath. When the contrast in the descending aorta reached 180 HU, imaging began. The axial pictures were acquired on a state-of-the-art Philips Brilliance workstation and then processed using techniques such maximum intensity projection, volume rendering, and curved and oblique (MPR) (VR). Axial pictures with a slice thickness of 0.6 mm were employed for the examination of the tiny and complex coronary arteries.

We selected the best phases (Avoid Artifacts). The axial pictures were then updated to evaluate the extra-cardiac structures, the opacification degree of the cardiac chamber as well as walls, and the cardiac anatomy. To fully identify the coronary anatomy, the coronary artery tree was examined in both axial and reconstructed pictures. To achieve reliable calculation of coronary bifurcation angles, they measured using both CMPR and 3D VR techniques at suitable plains (**Figures 1 and 2**). Also, the extent of coronary artery stenosis was measured, the related coronary plaques were localized and characterized, and the degree of CAD was

determined. Two radiologists with six and eleven years of expertise in cardiac imaging made the final diagnosis.

Ethical Consideration:

This study was ethically approved by the Institutional Review Board [IRB] of the Faculty of Medicine, Zagazig University (10576). Written informed consent was obtained from all participants. This study was executed according to the code of ethics of the World Medical Association (Declaration of Helsinki) for studies on humans.

Statistical Analysis

Data for the study was collected and analyzed using SPSS 20.0 (Statistical Package for Social Sciences). Qualitative data were reported as a number and a percentage, while quantitative data were presented as mean standard deviation (SD) or median and interquartile range (IQR) based on the results of normality testing. The significance of differences between quantitatively paired groups was examined using Paired t-test and Mann-Whitney U test. Data analysis additionally made use of MedCalc version 18.2.1. Coronary artery angle models were employed in the study to calculate age-related reference intervals. Finally, the study examined the inter-method agreement between VR and CMPR for measuring different coronary bifurcation angles using The Bland-Altman method.

RESULTS

A total of 60 of the 87 patients who underwent MDCT angiography were included in the study; there were 43 men (71.7% of the total) and 17 women (28.3%).

The patients' average age was 48.3 (SD 13.9) years, with ages ranging from 12 to 68. Patients between the ages of 50 and 60 made up the bulk of those selected (66%), while 21 children and 6 adults were omitted because of the bad image quality.

In order to obtain the most accurate data, we assessed various angles of coronary bifurcations in 60 patients using a variety of methodologies. Axial MIP images were used to assess the angle between the aorta and right coronary artery (Aorta-RCA), which showed a range of 23.6° to 129° with a mean of 75° (SD 26.2°) and to quantify the angle between the aorta and left main artery (Aorta-LMA), which ranged from 16° to 147.4° with a mean of 73.1° (SD 29.2°). Also, we split our 60 patients into two groups: the first group, which included 40 patients, in which the LMA bifurcates into left circumflex artery (LCX) and left anterior descending artery (LAD). The (Aorta-LMA) in this group ranged from 26.8° to 147.4°, whereas the 20 patients in the trifurcation group had angles ranging from 16° to 129°. No statistically significant difference existed between the two groups (**Table 1**).

Table (1): Comparison of different angles among bifurcation and trifurcation groups.

Variable	N	Mean	SD	Min-Max	Paired t-test	P-value
LMA-LAD-VR ^o (bifurcation)	40	148.3	16.49	103 – 177	1.741	0.078 (NS)
LMA-LAD-VR ^o (trifurcation)	20	140.04	18.40	114 – 179		
LMA-LCX-VR ^o (Bifurcation)	40	134.5	18.25	82 - 163	2.047	0.04 (S)
LMA-LCX-VR ^o (trifurcation)	20	122.7	24.41	73 - 159		
LAD-LCX-VR ^o (Bifurcation)	40	73.65	24.70	30.2 – 114	-4.115	<0.001 (HS)
LAD-LCX-VR ^o (Trifurcation)	20	100.36	21.23	70.8 - 143.8		
LAD-LCX-CMPR ^o (Bifurcation)	40	75.67	21.42	31.4 - 113.2	-3.810	<0.001 (HS)
LAD-LCX-CMPR ^o (Trifurcation)	20	98.23	21.71	67.9 - 141.2		

In order to get precise and trustworthy results, we evaluated the angle between the LMA bifurcation branches (LAD and LCX) in 40 patients using two different techniques: 3D VR and CMPR. When evaluated in 3D VR, the (LAD-LCX) angles varied from 30.2° to 114° with a mean of 75.4° (SD 21.5°), and from 31.4° to 113.2° with a mean of 75.6° (SD 21.4°) in CMPR (Table 2). A statistical comparison of the two methods for determining the angle between LAD and LCX in the bifurcation group indicated no statistically significant differences.

Table (2): Comparison of LAD-LCX angles by both VR and CMPR among bifurcation group.

Variable	N	Mean	SD	Min-max	Paired t-test	P-value
LAD-LCX-VR ^o	40	75.42	21.55	30.2 - 114	-0.836	0.763 (NS)
LAD-LCX-CMPR ^o	40	75.67	21.42	31.4 -113.2		

Using 3D VR and CMPR methods, we calculated the angles between the trifurcation group’s (LAD-RI), (LCX-RI), and (LAD-LCX). In 3D VR, the angles between the LAD and the LCX ranged from 70.8° to 143.8°, with a mean of 100.3° (SD 21.1°), while in CMPR, they ranged from 67.9° to 141.2°, with a mean of 98.2° (SD 21.7°). The statistical analysis revealed a substantial difference in the LAD-LCX angle measurement between the two methods, with a mean difference of 1.1 and limits of agreement ranging from -4.9° to 7.0°.

In terms of the LAD-RI angle, it varied from 21.9° to 81° with a mean of 44.7° (SD 16.2°) in CMPR and from 22.2° to 80.4° with a mean of 46.8° (SD 15.5°) in 3D VR. In contrast, there was no statistically significant difference in the measurement of the LCX-RI angle, which varied from 27.1° to 89.5° with a mean of 53.5° (SD 14.5°) in 3D VR and from 27° to 88.9° with a mean of 53.6° (SD 13.7°) in CMPR (Table 3).

Table (3): Comparison of different angles by both VR and CMPR among trifurcation group.

Variable	N	Mean	SD	Min-max	Paired t-test	P-value
LAD-LCX-VR ^o	20	100.36	21.13	70.8 – 143.8	3.131	0.005 (S)
LAD-LCX-CMPR ^o	20	98.23	21.71	67.9 – 141.2		
LAD-RAMUS-VR ^o	20	46.83	15.54	22.2 – 80.4	2.202	0.04 (S)
LAD-RAMUS-CMPR ^o	20	44.70	16.21	21.9 - 81		
LCX-RAMUS-VR ^o	20	53.51	14.53	27.1 – 89.5	-0.321	0.751 (NS)
LCX-RAMUS-CMPR ^o	20	53.68	13.77	27 – 88.9		

The 3D VR and CMPR approaches had good agreement in measuring the various coronary bifurcation angles, according to the Bland-Altman plot. As a result, both methods are interchangeable (Figure 3a).

There was a noticeable difference between the bifurcation group and the trifurcation group when

comparing the LAD-LCX angle, with the trifurcation group's angles being higher than the bifurcation group's. While the (LMA-LCX) angle was significantly smaller in the trifurcation group compared to the bifurcation group, the (LMA-LAD) angle exhibited no significant difference between both groups.

The results of comparing various coronary angles between patients with and without severe CAD are shown in **Table 4**. Both the LAD-LCX angle by VR (°) and by CMPR (°) showed statistically significant differences in coronary angles between the two groups (p-values of 0.007 and 0.014, respectively). As shown in **(Figure 3b)**, patients with substantial CAD had median (IQR) LAD-LCX angles that were higher [92 (78- 108) °] than those with non-significant CAD [74 (58-90)°],

and this was true for the trifurcation group as well as the bifurcation group.

The other coronary angles studied, however, showed no discernible variation. Whereas the best cutoff value for LAD-LCX angle in CMPR was >97° (sensitivity=47%, specificity=86%), while the optimum cutoff value for VR was found to be >74° (sensitivity=83%, specificity=52%) **(Figure 3c)**.

Table (4): Comparison of coronary artery angles in patients with or without significant CAD.

Variable	Non-significant CAD			Significant CAD			U	Z	P-value*
	N	Median	IQR	N	Median	IQR			
Aorta-RCA angle by axial MIP (°)	28	84	57 – 95	30	86	64 - 101	380.0	-0.622	0.534
Aorta-LMA angle by axial MIP (°)	27	72	50 – 87	29	70	50 - 94	381.0	-0.172	0.863
Aorta-LAD angle by axial MIP (°)	1	72	72 – 72	1	59	59 - 59	0.000	-1.000	0.317
LMA-LAD angle by VR (°)	26	147	135 -158	29	144	136 - 159	375.5	-0.025	0.980
LMA-LCX angle by VR (°)	26	137	127 -150	29	127	116 - 143	270.0	-1.804	0.071
LAD-LCX angle by VR(°)	27	74	58 – 90	30	92	78 - 108	236.0	-2.701	0.007
LAD-LCX angle by CMPR (°)	28	74	58 – 91	30	89	74 - 107	261.5	-2.466	0.014
LAD-ramus angle by VR (°)	5	37	36 – 51	14	47	39 - 56	22.0	-1.205	0.228
LAD-ramus angle by CMPR (°)	5	37	37 – 50	14	42	38 - 55	26.0	-0.834	0.405
LCX-ramus angle by VR (°)	5	54	52 – 64	14	48	43 - 62	25.0	-0.926	0.354
LCX-ramus angle by CMPR (°)	5	55	53 – 60	14	49	43 - 64	27.0	-0.741	0.459

Data are presented as median and interquartile range. IQR = interquartile range, N = number, U = *Mann-Whitney U test. Z = Z value.

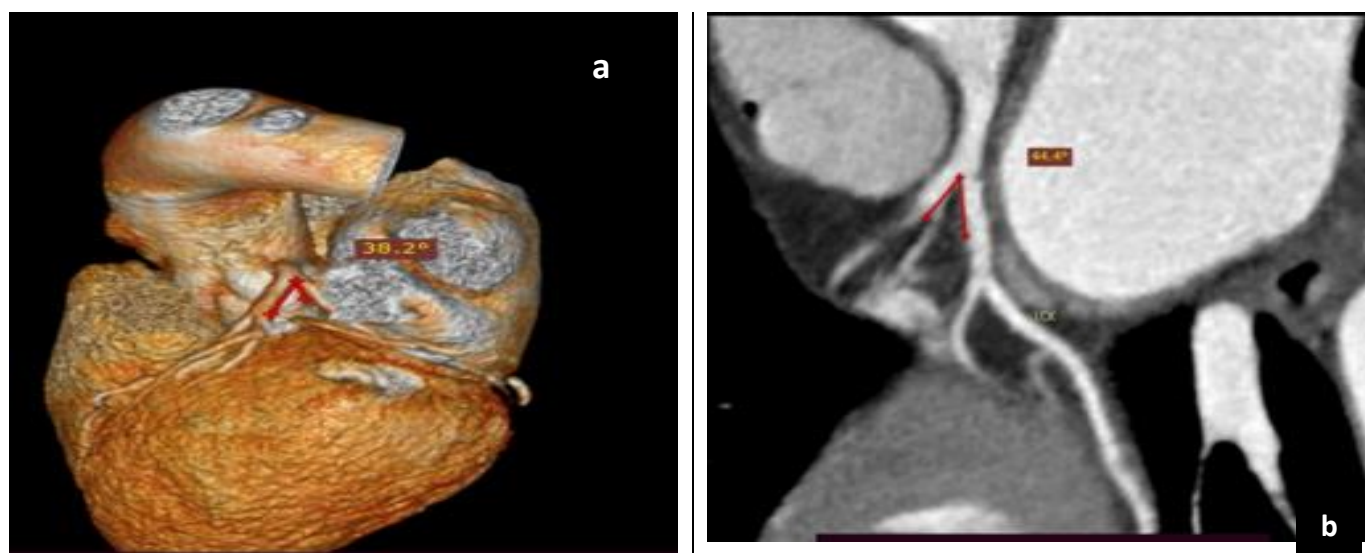


Figure (1): (a and b) showing LAD_LCX angle measured at VR (38.2°) and CMPR (44.4°) respectively in a case with no evidence of CAD.

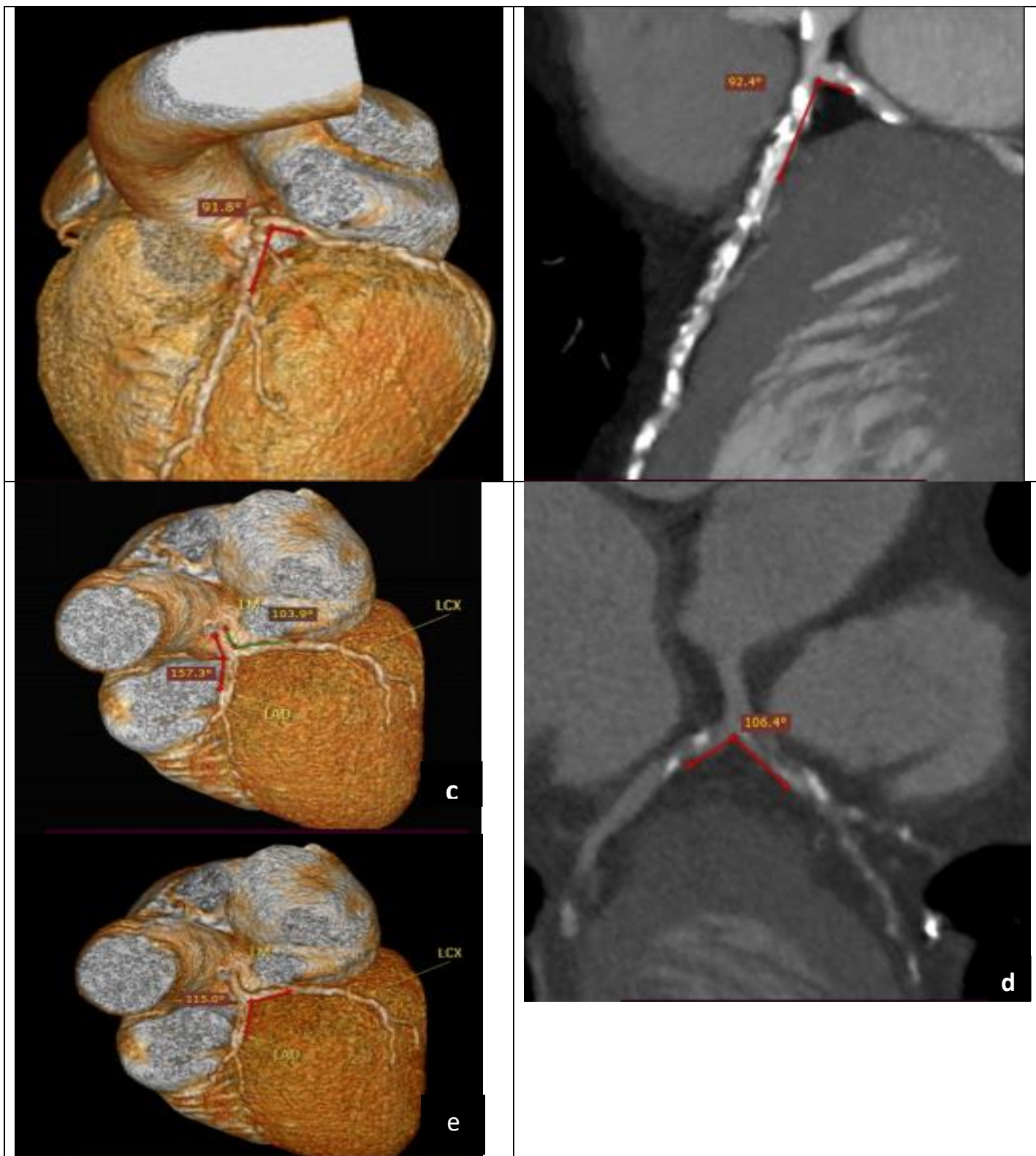


Figure (2): (a and b) showing LAD LCX angle measured at VR (91.8°) and CMPR (92.4°), respectively in patient with significant CAD. (c) 3D VR image demonstrating the measured LM-LAD (103.9°) and LM-LCX (157.3°) angles in another patient with CAD. (d and e) showing the LAD LCX measured in CMPR (106.4°) and at VR (115°), respectively in the same patient of C image.

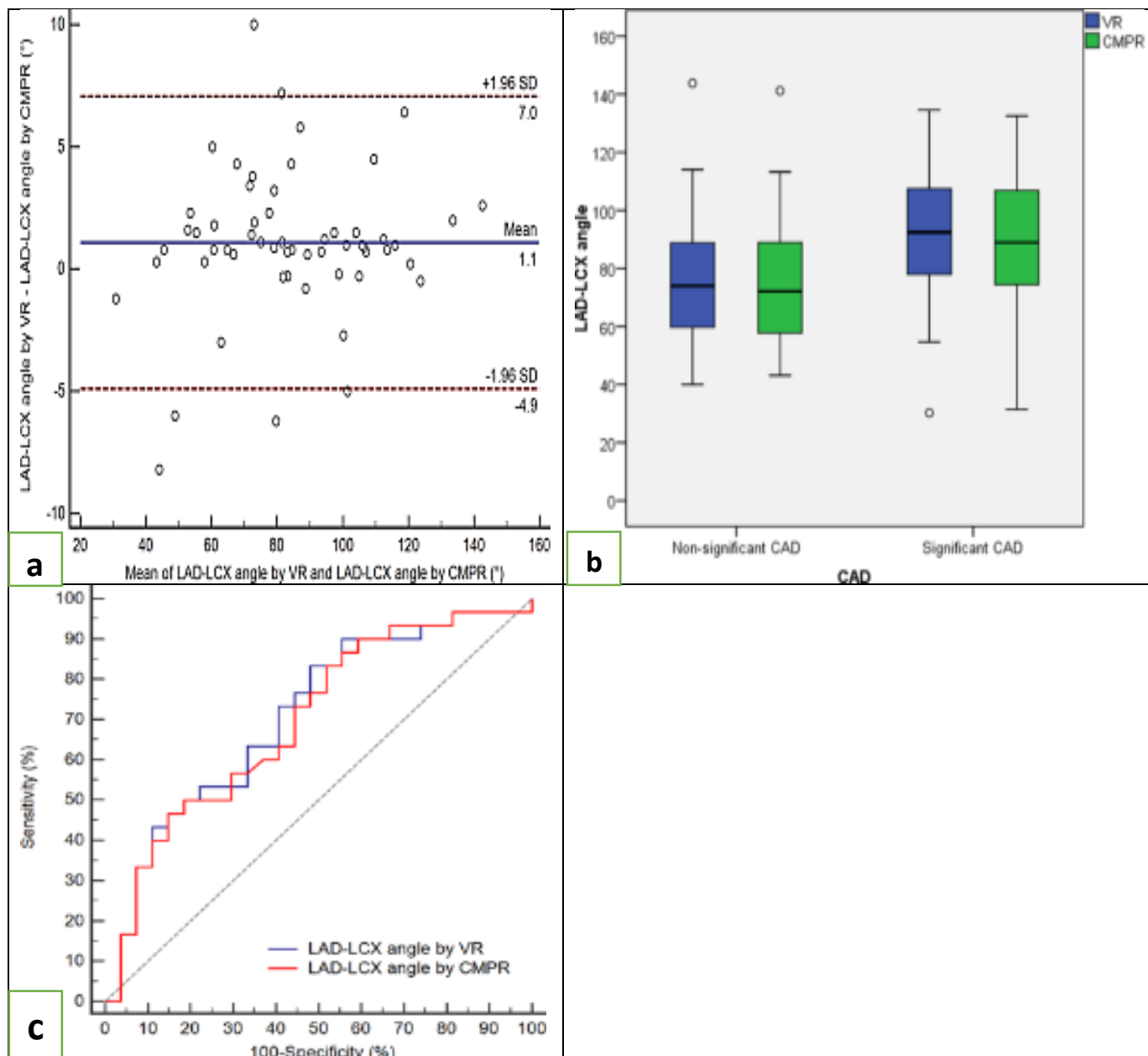
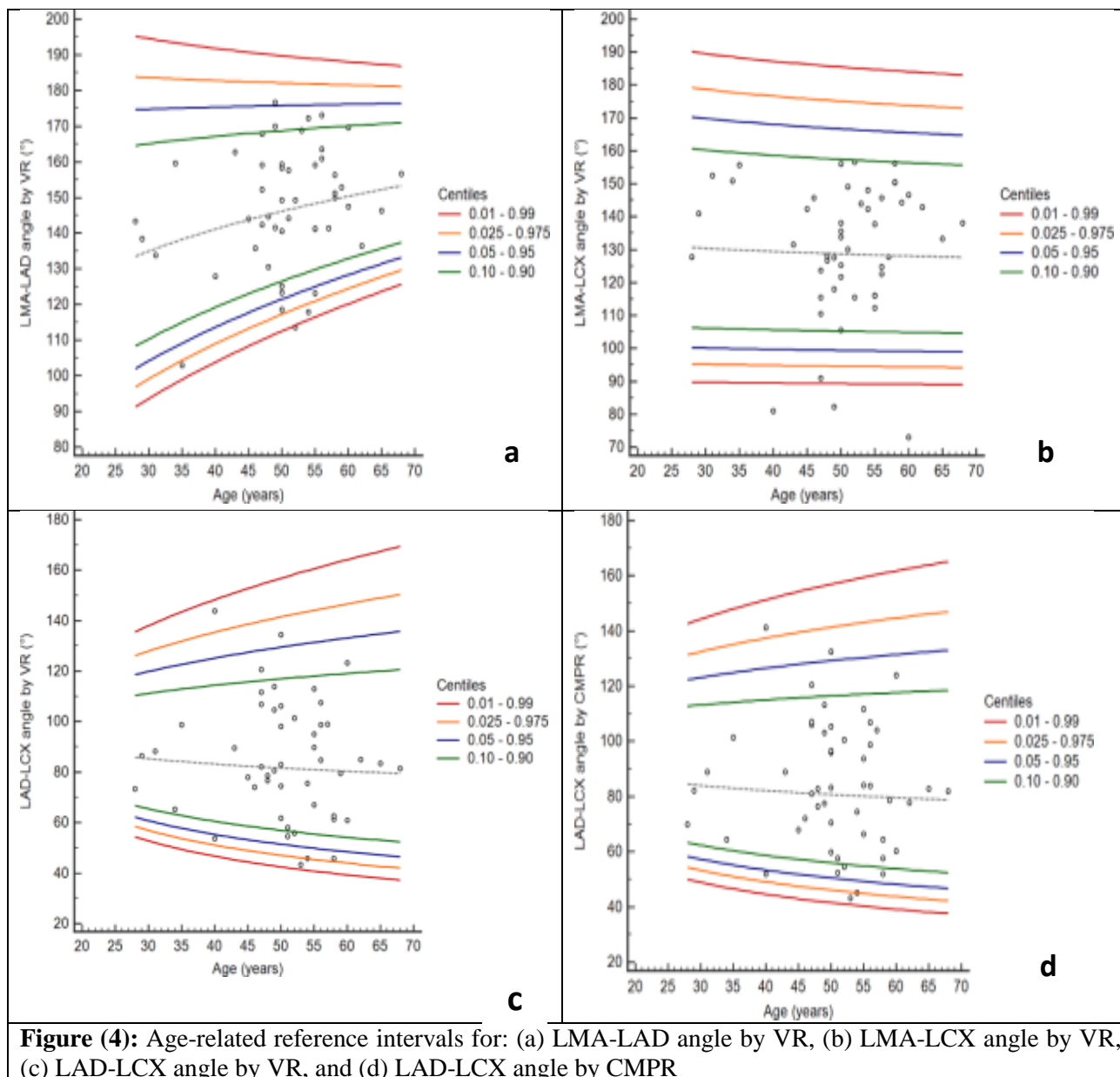


Figure (3): (a) Bland-Altman plot for agreement between VR and CMPR for measurement of the LAD-LCX angle. Bias= 1.1°, limits of agreement= -4.9° to 7.0°. (b) Box plot illustrating the LAD-LCX angle in patients who had or who were without significant CAD. Interquartile range is shown via box plot. The median is indicated by the horizontal line in the middle of the box. Whiskers denote the range of values outside the extremes (rounded markers). (c) Receiver-operating characteristic (ROC) curve to discriminate between cases with significant or non-significant CAD using LAD-LCX angle as measured with VR or CMPR. Best cutoff in VR is LAD-LCX angle >74° (sensitivity=83%, specificity=52%). Best cutoff in CMPR is LAD-LCX angle >97° (sensitivity=47%, specificity=86%).

In order to establish age-related reference intervals for various coronary angles, the study performed a correlation analysis between patient age and coronary angle measurements at both VR and CMPR procedures. The findings revealed that, irrespective of the measuring method, age-related reference intervals for various coronary angles were comparable. In particular, the age-related reference intervals for the LMA-LAD and LAD-RI angles measured by VR grew with age at both the 5th and 95th percentiles, while the gaps for the LMA-LCX and LCX RI angles somewhat shrank with age at the 5th-95th percentile. The study also discovered that the LAD-LCX angle's age-related reference intervals for both approaches altered with age (**Figure 4**).



DISCUSSION

CAD is often associated with the bifurcation angle of coronary arteries, as atherosclerotic plaques tend to form in areas of turbulent and slow blood flow near side branches. The LAD-LCX angle is a key branch in the development of CAD, with a larger angle indicating a greater risk of plaque buildup. CCTA is an effective and non-invasive diagnostic tool for CAD, and advancements in CT technology have made it possible to accurately measure the bifurcation angle using various image rendering and processing techniques.

With a variety of post-processing methods, such as CMPR and VR, our study intends to examine the capability of MDCT coronary angiography to estimate coronary angles. In a cohort of 60 patients, we also hope to establish a connection between the measured angles and the degree of CAD. The link between the LAD-LCx angle, degree of stenosis, and plaque features in CAD across a variety of patient demographics has also been investigated in earlier research.

Cui et al. [4] looked at 106 patients, whereas **Moon et al.** [6] and **Juan et al.** [10] analysed 201 and 313 patients, respectively. **Rodriguez Granillo et al.** [11] looked into plaque burden and its connection with bifurcation angle in 50 patients. Moreover, **Sun and Cao** [12] used CT angiography in 30 patients to investigate the relationship between the left coronary bifurcation and the onset of CAD. We observed that different methods were used in our study and **Givehchi et al.** [5] investigation to evaluate the bifurcation angles using coronary computed tomography angiography (CCTA).

Our study used 3D VR and CMPR images to measure the LAD-LCX angle values in the bifurcation and trifurcation groups and discovered no statistically significant differences between the two methods in the bifurcation group. The CMPR measured angle values, however, were statistically inferior to the 3D VR recorded angle values in the trifurcation group. In contrast, **Givehchi et al.** [5] used made-up phantoms to test the precision of MPR and VRT in determining the

bifurcation angle and discovered a strong correlation between the true and measured angles using both techniques. However, we discovered that the 3D VR measured angles in our study had higher values relative to their counterpunch CMPR measured angles in some angles, which deviated from their findings, even though we concur with their conclusion that both techniques showed a significant correlation to the true bifurcation angle.

In our work, we used CMPR and 3D VR techniques to compare the coronary bifurcation angles at LMA bifurcation and trifurcation groups. Although there was no statistically significant difference in LM-LCX or LAD-LCX angles between the two groups, there was a difference in LAD-LCX and LM-LCX angles. These findings are consistent with earlier researches by **Sun and Cao** and **Sun** [12-13] who utilized VR for left coronary bifurcation angle measuring, **Mieghem et al.** [14] who obtained the bifurcation angles by using MPR on CCTA images, **Sabarudin et al.** [15] and **Cui et al.** [4] who validated the bifurcation angle's clinical value in predicting severe coronary stenosis.

In this study, we compared various coronary angles in patients with substantial and non-significant coronary artery disease (CAD). Our results showed a statistically significant difference in the LAD-LCX angle between patients with substantial and non-significant CAD, as assessed by 3D VR and CMPR methods. Patients with substantial CAD had a statistically larger median LAD-LCX angle than those without significant CAD. Other coronary angles, however, showed no statistically significant variation. These findings are consistent with those made public by **Cui et al.** [4], **Juan et al.** [10], **Chaichana et al.** [16], **Ziyrek et al.** [17] and **Zhang et al.** [18] in addition to other investigations.

According to our findings, LAD-LCX angle $>74^\circ$ in substantial CAD employing VR is the optimum cutoff value, whereas LAD-LCX angle $>97^\circ$ in CMPR is the optimal cutoff. These results concur with those of **Cui et al.** [4], who determined a threshold value of 78 for predicting severe left coronary stenosis using LAD-LCx angle. The researchers **Juan et al.** [10] and **Temov et al.** [19] also discovered that a LAD-LCx angle of 80° is a threshold value for predicting left coronary stenosis. In addition, they discovered that, in comparison to females and patients with a low body mass index (BMI), men and patients with a high BMI had considerably higher odds of having a LAD-LCx angle $>80^\circ$.

In a different study, **Sun and Cao** [12] found that 89 percent of patients with LAD and LCx disease had a bifurcation angle >90 degrees, and in a subsequent study, found that patients with left coronary disease and a LAD-LCx angle >80 degrees had significantly larger mean LAD and LCx diameters than patients with left coronary disease and a LAD-LCx angle of 80 degrees. In contrast to the cutoff values in our investigation and previous studies, **Moon et al.** [6] determined a LAD-LCx

angle of 60° as a cutoff value for predicting left coronary stenosis.

In terms of the LM-LAD angle, our research revealed no discernible difference between patients with substantial and minimal CAD. However, the findings of **Moon et al.** [6] and **Konishi et al.** [21], An LM-LAD angle greater than 40 degrees is considered a threshold value for substantial CAD even with equal LAD-LCX angles, suggesting that the LM-LAD angle is a more accurate predictor of major LAD stenosis than the LAD-LCX angle.

Tsugu et al. [22] study's used MDCT coronary angiography to quantify the fractional flow reserve (FFR) of coronary arteries in individuals with non-apparent CAD. They discovered that the coronary bifurcation angle increases the risk of ischemia insult because the cutoff value of FFR at the distal segment of coronary vessels (such as the LAD) is less than 0.80 and this value falls as the angle increases. These results support our findings and show that coronary angle changes can serve as CAD predictors. These results were also validated by **Tsugu et al.** [23,24].

Finally, we used both VR and CMPR methods to investigate the relationship between patient age and coronary angles. Surprisingly, we discovered that the age-related reference intervals for various coronary angles were comparable.

In particular, we found that in both the 5th and 95th percentiles, the LMA-LAD and the LAD-ramus angles grew with age, whereas the LMA-LCX and the LCX-ramus angles shrank with age, while LAD-LCX angle is variable with age.

It's worth noting that previous studies did not provide a clear correlation between age and coronary angle measurements for comparison.

CONCLUSION

The study shows that employing post-processing methods like CMPR and 3D VR, CCTA can precisely quantify various coronary artery bifurcation angles. To determine whether CAD is likely, either method may be applied. According to the study, significant CAD rather than non-significant CAD is related with a greater LAD-LCx angle. However, because of the study's relatively limited sample size, no age connection with bifurcation angle values could be found. In order to define the age connection with each bifurcation angle and determine a cut-off value for each bifurcation angle, additional studies with a larger population size are advised.

Supporting and sponsoring financially: Nil.

Competing interests: Nil.

REFERENCES

1. **Cademartiri F, La Grutta L, Malagò R et al. (2008):** Prevalence of anatomical variants and coronary anomalies in 543 consecutive patients studied with 64-

- slice CT coronary angiography. *Eur Radiol.*, 18(4):781-91.
2. **Mehta R, Agarwal S (2013):** Evaluation of anatomic variations in coronary artery on 64-slice computed tomography angiography (CTA). *Int J Cur Res Rev.*, 5(15):23-30.
 3. **Tehrai M, Saidi B (2011):** A rare case of type IV dual left anterior descending artery and anomalous origin of the left coronary artery from the noncoronary sinus. *J Thorac Cardiovasc Surg.*, 142(2):451-2.
 4. **Cui Y, Zeng W, Yu J et al. (2017):** Quantification of left coronary bifurcation angles and plaques by coronary computed tomography angiography for prediction of significant coronary stenosis: A preliminary study with dual-source CT. *PLoS One*, 12(3):e0174352.
 5. **Givehchi S, Safari M, Tan S et al. (2018):** Measurement of coronary bifurcation angle with coronary CT angiography: A phantom study. *Phys Med.*, 45:198-204.
 6. **Moon S, Byun J, Kim J et al. (2018):** Clinical usefulness of the angle between left main coronary artery and left anterior descending coronary artery for the evaluation of obstructive coronary artery disease. *PLoS One*, 13(9):e0202249. doi: 10.1371/journal.pone.0202249
 7. **Rubinshtein R, Lerman A, Spoon D et al. (2012):** Anatomic features of the left main coronary artery and factors associated with its bifurcation angle: a 3-dimensional quantitative coronary angiographic study. *Catheter Cardiovasc Interv.*, 80:304-9.
 8. **Handran C, Garberich R, Lesser J et al. (2015):** The Left Main Bifurcation Angle and Changes Throughout the Cardiac Cycle: Quantitative Implications for Left Main Bifurcation Stenting and Stents. *J Invasive Cardiol.*, 27:401-4.
 9. **Guo W, Liu X, Gao Z et al. (2015):** Quantification of threedimensional computed tomography angiography for evaluating coronary luminal stenosis using digital subtraction angiography as the standard of reference. *Biomed Eng Online*, 14:50-5.
 10. **Juan Y, Tsay P, Shen W et al. (2017):** Comparison of the left main coronary bifurcating angle among patients with normal, non-significantly and significantly stenosed left coronary arteries. *Sci Rep.*, 7:1515-8.
 11. **Rodriguez-Granillo G, Rosales M, Degrossi E et al. (2007):** Multislice CT coronary angiography for the detection of burden, morphology and distribution of atherosclerotic plaques in the left main bifurcation. *Int J Cardiovasc Imaging*, 23:389-92.
 12. **Sun Z, Cao Y (2011):** Multislice CT angiography assessment of left coronary artery: Correlation between bifurcation angle and dimensions and development of coronary artery disease. *Eur J Radiol.*, 79:90-5.
 13. **Sun Z (2013):** Coronary CT angiography in coronary artery disease: correlation between virtual intravascular endoscopic appearances and left bifurcation angulation and coronary plaques. *Biomed Res Int.*, 2013:732059. doi: 10.1155/2013/732059
 14. **Van Mieghem C, Thury A, Meijboom W et al. (2007):** Detection and characterization of coronary bifurcation lesions with 64-slice computed tomography coronary angiography. *Eur Heart J.*, 28:1968-76.
 15. **Sabarudin A, Sun Z (2013):** Coronary CT angiography: diagnostic value and clinical challenges. *World J Cardiol.*, 5:473-83.
 16. **Chaichana T, Sun Z, Jewkes J (2011):** Computation of hemodynamics in the left coronary artery with variable angulations. *J Biomech.*, 44:1869-78.
 17. **Ziyrek M, Sertdemir A, Duran M (2020):** Effect of coronary artery bifurcation angle on atherosclerotic lesion localization distance to the bifurcation site. *J Saudi Heart Assoc.*, 32:399-407.
 18. **Zhang B, Jin Y, Wang X et al. (2017):** Numerical simulation of transient blood flow through the left coronary artery with varying degrees of bifurcation angles. *J Mech Med Biol.*, 17:1750005. doi: 10.1142/S0219519417500051
 19. **Temov K, Sun Z (2016):** Coronary computed tomography angiography investigation of the association between left main coronary artery bifurcation angle and risk factors of coronary artery disease. *Int J Cardiovasc Imaging*, 32:129-37.
 20. **Craiem D, Casciaro M, Graf S et al. (2009):** Coronary arteries simplified with 3D cylinders to assess true bifurcation angles in atherosclerotic patients. *Cardiovasc Eng.*, 9:127-33.
 21. **Konishi T, Yamamoto T, Funayama N et al. (2016):** Relationship between left coronary artery bifurcation angle and restenosis after stenting of the proximal left anterior descending artery. *Coron Artery Dis.*, 27:449-59.
 22. **Tsugu T, Tanaka K, Nagatomo Y et al. (2023):** Impact of coronary bifurcation angle on computed tomography derived fractional flow reserve in coronary vessels with no apparent coronary artery disease. *Eur Radiol.*, 33(2):1277-85.
 23. **Tsugu T, Tanaka K (2022):** Differences in fractional flow reserve derived from coronary computed tomography angiography according to coronary artery bifurcation angle. *Turk Kardiyol Dern Ars.*, 50:83-4.
 24. **Tsugu T, Tanaka K, Belsack D et al. (2021):** Impact of vascular morphology and plaque characteristics on computed tomography derived fractional flow reserve in early stage coronary artery disease. *Int J Cardiol.*, 343:187-93.